

RECENT RESULTS FROM THE CMD-2 DETECTOR AT THE VEPP-2M COLLIDER

E. P. Solodov

Budker Institute of Nuclear Physics, Novosibirsk, 630090, Russia

Representing the CMD-2 Collaboration

ABSTRACT

The general-purpose detector CMD-2 is taking data at the Novosibirsk VEPP-2M e^+e^- collider in the energy range 360–1400 MeV, with luminosity of $\approx 5.0 \times 10^{30} \text{ cm}^{-2} \text{ s}^{-1}$ for the ϕ resonance region. Data from $\approx 1500 \text{ nb}^{-1}$ of integrated luminosity around 1.02 GeV and $\approx 500 \text{ nb}^{-1}$ in the 600–1000 MeV range have been collected and preliminary analyses performed. We present progress in studies of the ϕ meson and $K_S K_L$ systems:

- (a) measurement of the ϕ meson parameters;
- (b) searches for ϕ rare decays. The new upper limits $B(\phi \rightarrow \eta' \gamma) < 2.4 \times 10^{-4}$, $B(\phi \rightarrow \pi^+ \pi^- \pi^+ \pi^-) < 1.0 \times 10^{-4}$, and $B(\phi \rightarrow f_0 \gamma) < 8 \times 10^{-4}$ have been obtained;
- (c) the study of the K_L interactions in the CsI calorimeter;
- (d) with the help of 32,340 tagged K_S , the semi-rare decay of $K_S \rightarrow \pi^+ \pi^- \gamma$ has been observed with a branching ratio of $(1.82 \pm 0.49) \times 10^{-3}$; and
- (e) selection of events with $K_S K_L$ coupled decays and interactions. The regeneration cross section of the low momenta K_L was found to be $\sigma_{reg}^{Be} = 63 \pm 19 \text{ mb}$.

Data from the 600–1000 MeV energy range are used for high-accuracy measurement of the e^+e^- annihilation cross section, and the preliminary analysis is presented in this paper.

1 Introduction

The VEPP-2M collider at the Budker Institute of Nuclear Physics in Novosibirsk, Russia, shown in Fig. 1, covers the center-of-mass energy range from the two-pion threshold up to 1400 MeV (Ref. 1). Experiments at this collider yielded a number of important results in e^+e^- physics, including the most precise pion form factor measurements² and studies of the ϕ , ω , and ρ meson decays.^{3,4} During 1988-92, it was upgraded to allow higher positron currents and injection of the electron and positron beams directly at the beam energy, rather than at lower energies and acceleration after injection. After installation of the new booster, VEPP-2M has peak luminosity $L \approx 5.0 \times 10^{30} \text{ cm}^{-2}\text{s}^{-1}$ at 40 mA per beam at the ϕ center-of-mass energy.

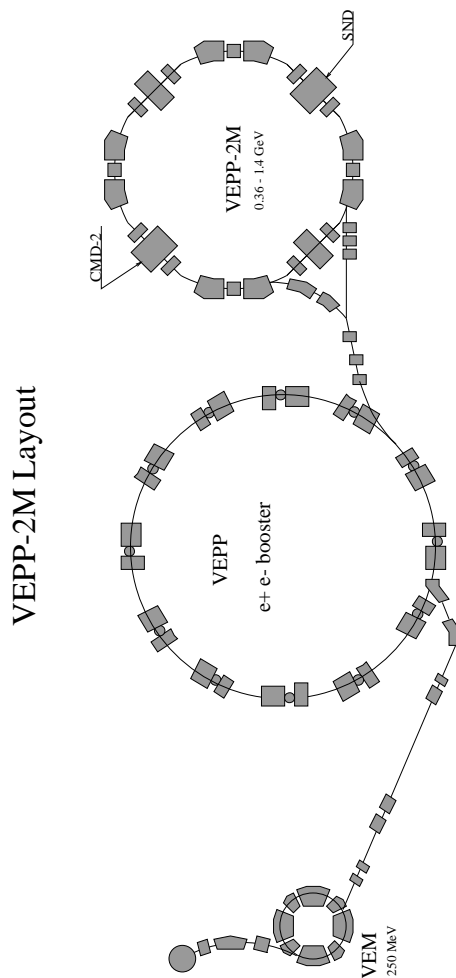


Fig. 1. The layout of the VEPP-2M collider at the Budker Institute of Nuclear Physics in Novosibirsk.

In this paper, we present some preliminary results from two energy regions: one is the relatively narrow region around the ϕ meson resonance, and the second is the region from 600 to 1000 MeV, essential for the measurements of the total hadron cross section in the VEPP-2M energy range.

2 Physics Motivation

The physics program of the CMD-2 detector is very rich; below we consider only some of the many aspects of the ϕ meson, and the total cross section of the e^+e^- annihilation into hadrons which will be studied.

As realized at the very early stages of the ϕ meson studies at colliding beam machines, $K_S K_L$ pairs ($\approx 34\%$ of all ϕ decays) may be used as a new source for observing CP and CPT violation. These suggestions, including studies of quantum mechanical correlations, were discussed in papers^{5,6} when the electron-positron collider at Novosibirsk VEPP-2M was under construction. The coupled decays of the $K_S K_L$ mesons will allow the demonstration of the quantum mechanical correlations of the two particle decays (Einstein-Podolsky-Rosen paradox).⁷

The idea of constructing a more intensive source of ϕ mesons has been discussed by many authors.^{8,9} The flux of events at these so-called “ ϕ -factories,” now under construction,^{10,11} will provide an opportunity to make new precise measurements of a possible direct component in the decay of the $K_L \rightarrow \pi^+\pi^-$, $\pi^0\pi^0$ (ϵ'/ϵ), as well as the observation of the CP-violating three pion decays of the K_S for the first time. The study of the oscillations in the joint decay distributions could give information about real and imaginary parts of any CPT-violating amplitude.

At the VEPP-2M collider, which could be considered as a pre- ϕ -factory, with the CMD-2 detector, we have been proceeding step-by-step to prepare for work at the ϕ -factory which is now under construction. Studies of upgraded detectors and accelerators are in progress, including an intermediate $\approx 10^{32}$ luminosity collider for investigating the use of round beams, an important ingredient in the planned Novosibirsk ϕ -factory project.^{12,13}

With the CMD-2 detector, the neutral kaons from ϕ decays are under study, and the coupled $K_S K_L$ decays have been observed for the first time. The attempt to select the $K_L \rightarrow \pi^+\pi^-$ decays again emphasized problems with the semileptonic decay mode background as well as a high level of neutral kaon nuclear interactions, including regeneration of K_L into K_S . The opening of this kinematic region for the neutral kaon interactions study has been an additional argument for the construction of ϕ -factories, and we anticipate that the results obtained from the

data now in hand will be important in planning for ϕ -factory detectors and for physics strategies.

A possible problem with a measurement of ϵ'/ϵ at the level of 10^{-4} – 10^{-5} would be an admixture of $C = +1$ into the final state, giving a component of $K_S K_S$ instead of the desired $K_S K_L$. Although efficient experimental cuts can reduce the effects of such an admixture,^{14,15} a component as large as 5×10^{-5} of a $C = +1$ state would give a dominant contribution to the uncertainty of ϵ'/ϵ at the level of the planned ϕ -factory experiments.¹⁵ The contamination from such a C -even $K\bar{K}$ mode has been estimated by several authors as giving generally lower values,^{8,16–18} but there are no experiments confirming these results.

The decay of the $\phi \rightarrow f_0 \gamma$ with f_0 decaying to two kaons is too small to be seen at the VEPP-2M collider, and we hope to study the decay of $\phi \rightarrow f_0 \gamma$ with a subsequent decay of the f_0 to two charged pions.¹⁹ The two charged pion decay mode can be related to the two kaon decay and a limit on the C -even two kaon final state may be found. Estimates for the branching ratio of $\phi \rightarrow f_0 \gamma$ range from very small to as high as 2.5×10^{-4} (Refs. 16–18).

The study of the f_0 is interesting by itself. The 20% decay probability into a two kaon final state seems puzzlingly high if f_0 is a member of the $S = 0$ and $I = 0$ meson nonet. Various explanations for this large coupling to kaons have been advanced,^{16–18,20} including the idea that f_0 is really made of four quarks, with a “hidden strangeness” component: ($f_0 = s\bar{s}(u\bar{u} + d\bar{d})/\sqrt{2}$), or that it may be a $K\bar{K}$ molecule. A limit from VEPP-2M will help to distinguish between these different possibilities.

With expected high luminosity at the ϕ -factories, rare decay modes of ϕ can be measured with high accuracy. For example, a measurement of the $B(\phi \rightarrow \eta' \gamma)$ would give important information about quark structure of light mesons and possible contributions from gluonium states (if any). Our new data obtained with the present statistics already improve upper limits for this process, as well as for $\phi \rightarrow \pi^+ \pi^- \pi^+ \pi^-$ and $\phi \rightarrow f_0 \gamma$.

The data from the low-energy region from two pion production threshold up to 1400 MeV (maximum energy provided by VEPP-2M) are important both for the search of rare decays of the light vector mesons and for the calculation of the dispersion integral that relates the cross section of $e^+ e^-$ annihilation into hadrons to the value of the hadronic vacuum polarization. This value plays an important role in the interpretation of the fundamental Standard Model parameters and the evaluation of the anomalous magnetic moment of the muon,^{21,22} which will be measured in the E821 experiment at BNL with an extremely high precision of

0.35 ppm. To evaluate the contribution of the hadronic vacuum polarization to the muon g-2 with the same accuracy, a systematic error in hadronic cross section should be less than 0.5%, because the total hadronic muon contribution to g-2 was recently re-evaluated and was found to be 72 ± 1.6 ppm (Ref. 23). The main part of this contribution comes from the energy range which is provided by the VEPP-2M collider. The data on the cross section $e^+e^- \rightarrow \pi^+\pi^-$ in the energy range between ρ and Φ mesons were obtained with the CMD-2 detector, and a preliminary analysis is presented in this paper.

3 The CMD-2 Detector

The CMD-2 detector has been described in more detail elsewhere.^{6,24} The main systems of the detector are shown in Fig. 2.

The CsI barrel calorimeter with $6 \times 6 \times 15$ cm³ crystal size is placed outside a 0.4 r.l. superconducting solenoid with a 1 Tesla azimuthally symmetric magnetic field. The endcap calorimeter is made of $2.5 \times 2.5 \times 15$ cm³ BGO crystals and was not installed for the data presented here. The drift chamber inside the solenoid has about 250 μ resolution transverse to the beam and 0.5–0.6 cm longitudinally. The muon range system uses the streamer tubes and has 1–3 cm spatial resolution.

The collected sample of the Bhabha events was used for the calibration and determination of the reconstruction efficiency in the drift chamber and in the calorimeter. A momentum resolution of 6–8% for 500 MeV/c charged particles and energy resolution of about 10% for gammas in the CsI calorimeter have been obtained.

The integrated luminosity collected in 1992–1993 at ϕ was mostly used for the detector study and software development. Not all detector systems were running properly, and data presented here are still preliminary—better detector understanding and better reconstruction programs available now will give results with less systematic errors.

About 7.2×10^7 triggers were recorded at the ϕ meson region. The total integrated luminosity, determined by selection of Bhabha events, was found to be 1500 nb⁻¹.

The largest part of the integrated luminosity (≈ 1200 nb⁻¹ in the 14 energy points around ϕ mass) has been collected during the 1993 summer runs and was used for studies of rare decay modes of ϕ , coupled decays in the $K_S K_L$ system, and nuclear interactions of neutral kaons.

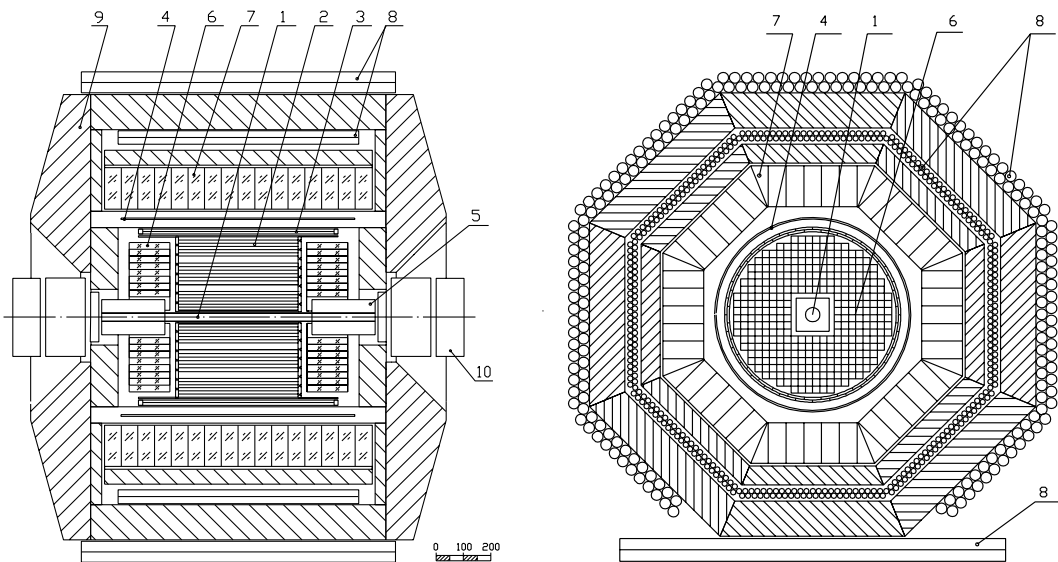


Fig. 2. Horizontal and vertical cross sections of the CMD-2 detector. (1) vacuum chamber; (2) drift chamber; (3) Z-chamber; (4) main solenoid; (5) compensating solenoid; (6) storage ring lenses; (7) calorimeter; (8) muon range system; and (9) magnet yoke.

The 1994–1995 runs were dedicated mostly to measurements of the total hadronic cross section at the energies below ϕ resonance. The integrated luminosity about $\approx 500 \text{ nb}^{-1}$ was collected; the experimental conditions are described below.

4 ϕ Meson Parameters

The main branching ratios of the ϕ have been measured using $\approx 300 \text{ nb}^{-1}$ of integrated luminosity, collected in 1992. It was the first time when four major decay modes of ϕ were measured in one experiment. The event selection and other details may be found in Ref. 25. The following results were obtained:

$$\begin{aligned}
 m_\phi &= 1019.380 \pm 0.034 \pm 0.048 \text{ MeV}, \\
 \Gamma_{tot} &= 4.409 \pm 0.086 \pm 0.020 \text{ MeV}, \\
 \sigma(\phi \rightarrow K^+K^-) &= 1993 \pm 65 \pm 82 \text{ nb}, \\
 \sigma(\phi \rightarrow K_S K_L) &= 1360 \pm 25 \pm 49 \text{ nb}, \\
 \sigma(\phi \rightarrow 3\pi) &= 656 \pm 24 \pm 30 \text{ nb}, \\
 \sigma(\phi \rightarrow \eta\gamma) &= 47.9 \pm 3.5 \pm 3.2 \text{ nb}, \text{ and} \\
 \delta_{\omega-\phi} &= (147 \pm 16)^\circ.
 \end{aligned}$$

The first error represents the uncertainty, and the second the systematic uncertainty. The relative phase of $\omega - \phi$ mixing in the three pion channel is in good agreement with the most precise measurement presented in Ref. 4, where $\delta_\phi = (155 \pm 15)^\circ$. The experimental cross sections of the ϕ production in the different modes, together with fit functions, are shown in Fig. 3.

All the major decay modes were simultaneously measured in one experiment; therefore, the branching ratios can be obtained as ratios of integrals over excitation curves independently of the width of the ϕ . The uncertainties due to the luminosity measurements are:

$$\begin{aligned}
 B(\phi \rightarrow K^+K^-) &= 49.1 \pm 1.2\%, \\
 B(\phi \rightarrow K_S K_L) &= 33.5 \pm 1.0\%, \\
 B(\phi \rightarrow 3\pi) &= 16.2 \pm 0.8\%, \\
 B(\phi \rightarrow \eta\gamma) &= 1.18 \pm 0.11\%.
 \end{aligned}$$

The electron width of the ϕ and its branching ratio to e^+e^- can also be calculated independently and were found to be

$$\begin{aligned}\Gamma_{ee} &= 1.27 \pm 0.05 \text{ keV}, \\ B(\phi \rightarrow ee) &= (2.87 \pm 0.09) \times 10^{-4}.\end{aligned}$$

All results are consistent with Particle Data Group values.²⁹

Here, we note that in all parameters, systematic errors dominate, and using all available statistics will improve these results only after systematic errors have been studied and there is better understanding of the detector.

5 Study of $\phi \rightarrow \eta\gamma$ and Search for $\eta'\gamma$

The decay of $\phi \rightarrow \eta\gamma$ was previously observed in neutral modes ($\eta \rightarrow \gamma\gamma$, $\eta \rightarrow 3\pi^0$) only. Detector CMD-2 gives the possibility to study $\phi \rightarrow \eta\gamma$ decay in the channel with charged particles, when η decays into $\pi^+\pi^-\pi^0$. So, after $\pi^0 \rightarrow \gamma\gamma$ decay, the final state consists of two charged pions and three photons. Two photons in the final state are from π^0 ; the third one has the maximum energy of all three—362 MeV at the ϕ meson peak.

We select $\eta\gamma$ events using the information about momenta and angles from the Drift Chamber for both charged particles and about an angle from the CsI calorimeter for a primary photon assuming that other photons are from π^0 . The reconstructed invariant mass of three pions $M_{\pi^+\pi^-\pi^0}$ is the basic parameter we use to study the decay $\phi \rightarrow \eta\gamma$, and the distribution over it should have a peak around $M_\eta = 547.45$ MeV.

The distribution over $M_{\pi^+\pi^-\pi^0}$ for all 1993 ϕ meson data after some simple cuts is presented in Fig. 4. These distributions were used to get the numbers of $\eta\gamma$ events for the different beam energies.

The calculated cross section $\sigma_{e^+e^- \rightarrow \phi \rightarrow \eta\gamma}$ with a fit function is presented in Fig. 4. Using the electron width of ϕ from Ref. 29, the $Br(\phi \rightarrow \eta\gamma)$ was found to be:

$$Br(\phi \rightarrow \eta\gamma) = (1.12 \pm 0.06 \pm 0.15)\%.$$

This result is preliminary because the work on efficiency determination is not yet complete, and we hope to significantly decrease the systematic errors.

The decay $\phi \rightarrow \eta'\gamma$ was searched in the mode, where η' decays into $\pi^+\pi^-\eta$ and $\eta \rightarrow \gamma\gamma$. So in both $\eta\gamma$ and $\eta'\gamma$ final states, there are two charged particles

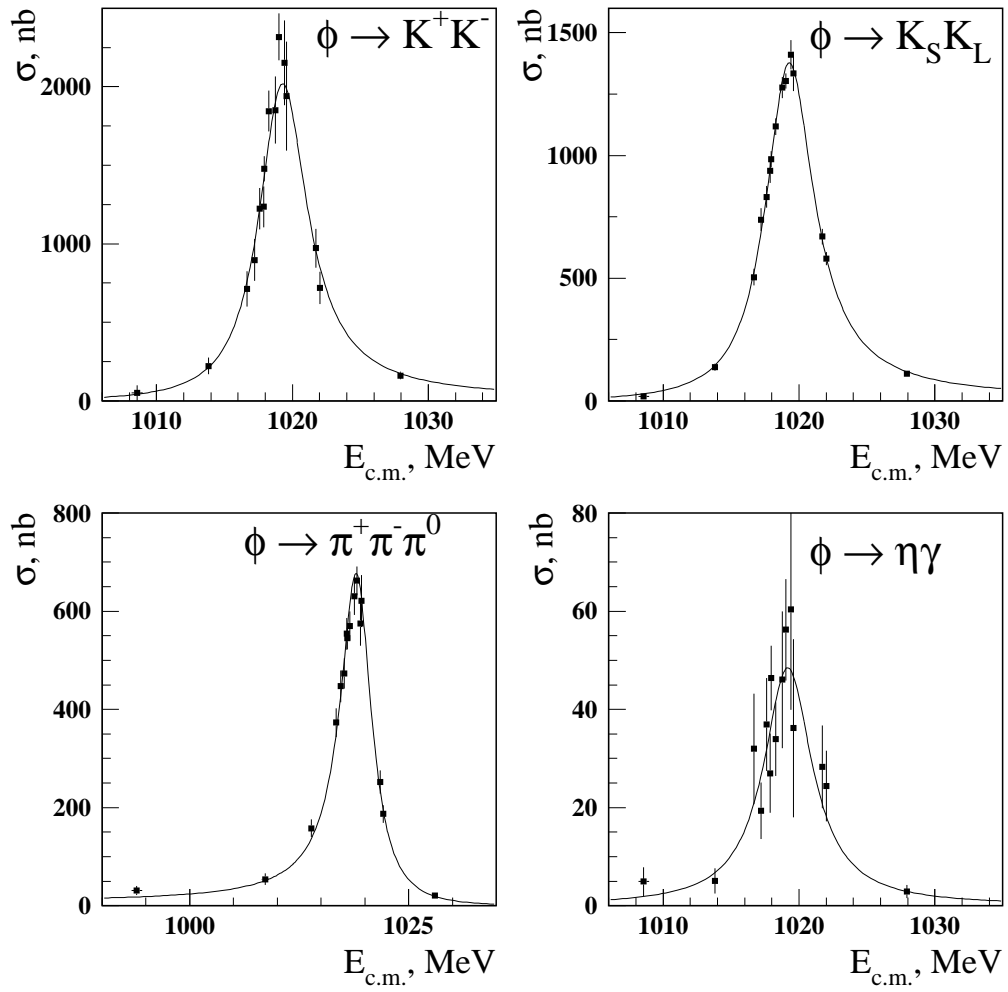


Fig. 3. The excitation curves for ϕ mesons in different channels.

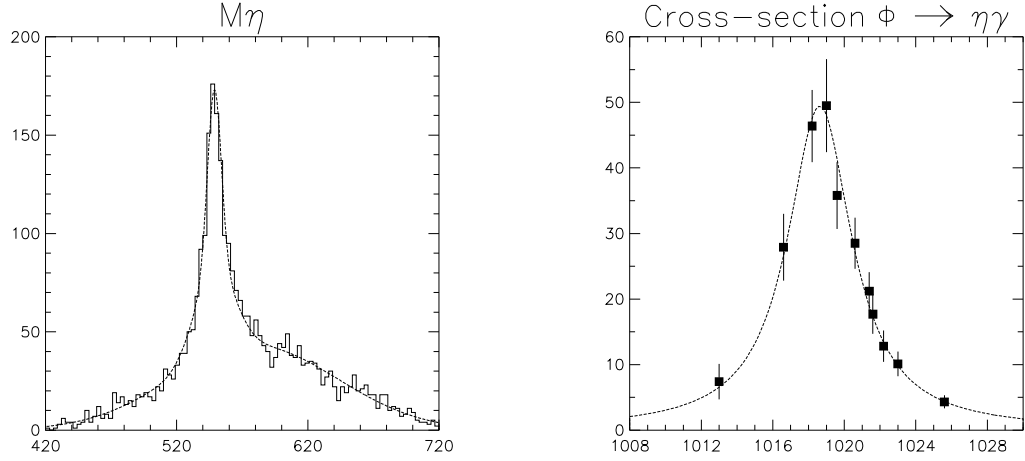


Fig. 4. The study of $\phi \rightarrow \eta\gamma$; invariant mass $M_{\pi^+\pi^-\pi^0}$ and $\phi \rightarrow \eta\gamma$ cross section.

and three photons. The events with all these detected particles were used for the constrained fit.

The scatter plot of the invariant masses for two soft photons M_{23} vs. the hardest photon energy ω_1 for the experimental data is presented in Fig. 5.

The decay into $\eta\gamma$ is the main background for $\eta'\gamma$. Removing the 481 $\eta\gamma$ events from the sample, the scatter plot of the invariant masses for the two hardest photons M_{12} vs. the weakest photon energy ω_3 was studied. For $\eta'\gamma$ events, M_{12} should be around η mass 547.5 MeV, while ω_3 is a monochromatic 60 MeV photon. Figure 5 presents the result of the 1992–1993 data together with simulation of $\phi \rightarrow \eta'\gamma$. We have one candidate $\eta'\gamma$ event, with one event estimated as the background. Using for the 90% C.L. upper limit $N_{\eta'\gamma} < 3$ and the ratio

$$\frac{Br(\phi \rightarrow \eta'\gamma)}{Br(\phi \rightarrow \eta\gamma)} = \frac{N_{\eta'\gamma}}{N_{\eta\gamma}} \cdot \frac{Br(\eta \rightarrow \pi^+\pi^-\pi^0)}{Br(\eta' \rightarrow \pi^+\pi^-\eta)} \cdot \frac{Br(\pi^0 \rightarrow \gamma\gamma)}{Br(\eta \rightarrow \gamma\gamma)} \cdot \frac{\varepsilon_{\eta\gamma}}{\varepsilon_{\eta'\gamma}},$$

with the efficiencies obtained from the simulation, $\varepsilon_{\eta\gamma} = 14.4\%$ and $\varepsilon_{\eta'\gamma} = 6.4\%$, the following result has been obtained:

$$Br(\phi \rightarrow \eta'\gamma) < 2.4 \times 10^{-4}.$$

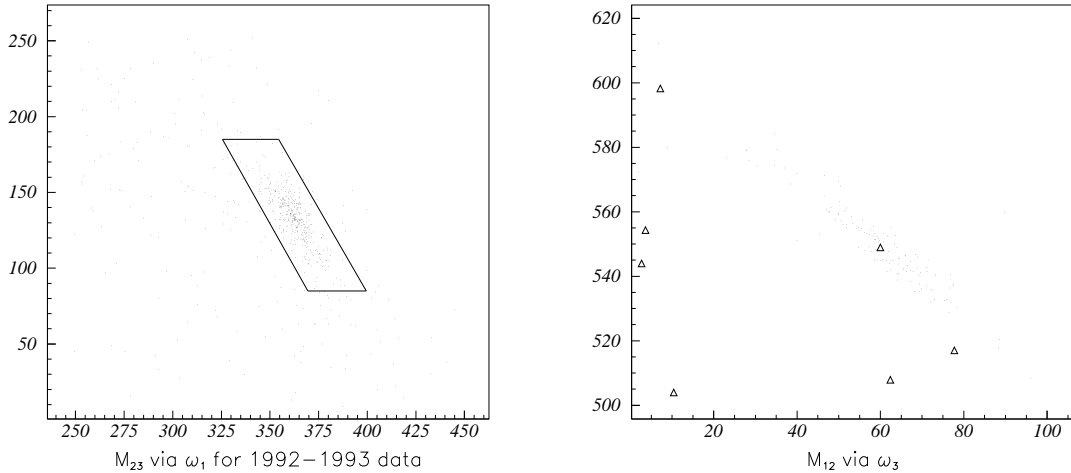


Fig. 5. The search for $\phi \rightarrow \eta' \gamma$ (1992–1993 data). Invariant mass M_{23} vs. ω_1 after the constrained fit (the box shows the $\eta \gamma$ cut); invariant mass M_{12} vs. ω_3 after constrained fits (dots are simulation, triangles the experiment).

6 Search for $\phi \rightarrow \pi^+ \pi^- \pi^+ \pi^-$

A sample of three- and four-track events was used to search for the process $\phi \rightarrow \pi^+ \pi^- \pi^+ \pi^-$. In this sample, tracks have to originate from the beam-beam interaction point within 0.5 cm in the r - ϕ plane and have at least nine hits in the Drift Chamber. The total charge has to be ± 1 for three-track events and zero for four-track events. To suppress background from the two-particle production and cosmic rays with some additional tracks, we reject events with at least two collinear tracks (mutual angle of any pair should be 0.16–3.0 rad in the r - ϕ plane).

Even with these selection criteria, we have a high background from the main channels of ϕ decaying into three-track events. So, in the search for the process $\phi \rightarrow \pi^+ \pi^- \pi^+ \pi^-$, only four-track events were used. The ratio of three- and four-track events at the energy points outside the ϕ meson region was used (along with simulation) for evaluation of a detection efficiency.

The scatter plot E_{tot} vs. P_{tot} for the selected four-track events is shown in Fig. 6. Here, P_{tot} is the magnitude of the total momentum of four charged particles, and E_{tot} is their total energy, assuming that all particles are pions. To extract

the number of events of the process $e^+e^- \rightarrow \pi^+\pi^-\pi^+\pi^-$, we apply a simple cut, shown in Fig. 6 as the box.

The extracted cross section vs. energy for the process $e^+e^- \rightarrow \pi^+\pi^-\pi^+\pi^-$ is also shown in Fig. 6. Only statistical errors are shown. A four-parameter function which contains linear background, amplitude, and phase of the process $\phi \rightarrow \pi^+\pi^-\pi^+\pi^-$ was used for the fitting. The result of the fit is shown in the plot by a smooth line. Using this fit and the uncertainty in the efficiency, one can get

$$Br(\phi \rightarrow \pi^+\pi^-\pi^+\pi^-) < 1.0 \times 10^{-4} \text{ for } C.L. = 90\% \quad .$$

This preliminary result is about nine times lower than the present upper limit for this process.²⁹ We plan to perform more simulations to improve both efficiency evaluation and data selection. Also, we plan to evaluate and apply radiative corrections which are about 5%.

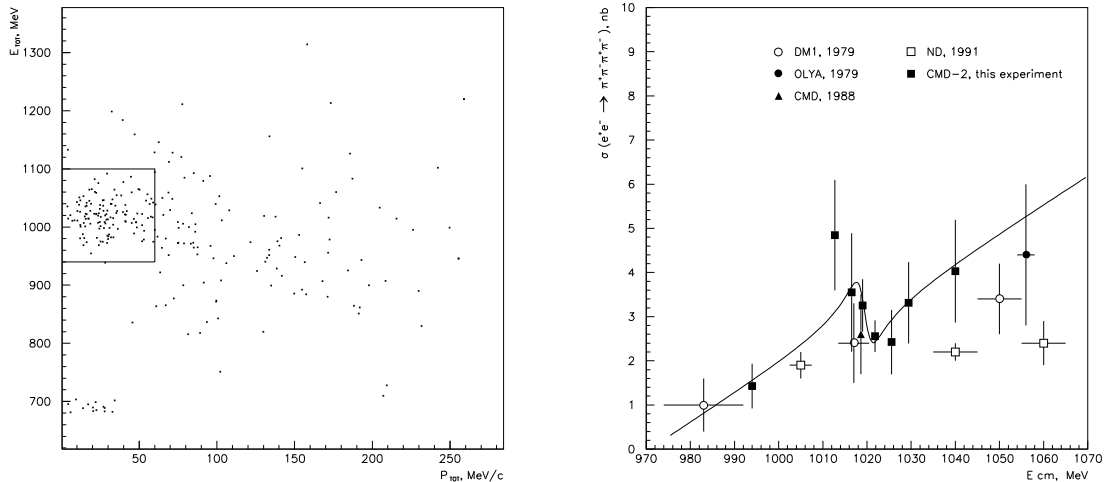


Fig. 6. The search for $\phi \rightarrow \pi^+\pi^-\pi^+\pi^-$. E_{tot} vs. P_{tot} for four-track candidates; cross section $e^+e^- \rightarrow \pi^+\pi^-\pi^+\pi^-$.

7 Search for $\phi \rightarrow f_0\gamma$

In order to extract the resonant contribution associated with the ϕ , two data sets were used. Energy points at $E_{c.m.}$ from 1016–1023.2 MeV with the integrated luminosity 660 nb^{-1} were used for the ϕ region, and points at $E_{c.m.} = 996, 1013,$

1026, 1030, and 1040 MeV with the integrated luminosity 440 nb^{-1} were used for a background estimation (the “non- ϕ ” region). The event candidates were selected by a requirement of only two charged tracks and only one photon with energy greater than 20 MeV in the detector. Total energy deposition was required to be less than 600 MeV, the average momentum of two charged tracks to be higher than 240 MeV, and the radial distance of the found vertex from the interaction region to be less than 0.15 cm. These cuts removed Bhabha events as well as charged and neutral kaons from ϕ decays. The requirement that the Z-coordinate of the vertex be within 10 cm at the detector center reduces cosmic ray background by a factor of two.

Each charged track was required to have a corresponding cluster in the calorimeter. This requirement reduced the number of pions by about 14% and helped avoiding nuclear interactions of the pions before the calorimeter with clusters in the wrong place. However, split clusters may still be present.

The main visible background for the studied process is $\phi \rightarrow \pi^+\pi^-\pi^0$ decay, when one of the photons from π^0 escapes detection. To reduce this background, a constrained fit was used. This fit required total energy and momentum conservation within detector resolutions for the three-body decay. For $\chi^2/\text{d.f.}$ less than three, only events with these requirements survived. But a three-pion background was still present, when one of the gammas from the π^0 had a very low energy and the event looked like a three-body decay. Figure 7 shows the spectrum of single gammas and the squared missing mass of two charged tracks (taken as pions) vs. detected gamma energy.

In the “ ϕ region” data sample, a broad peak at 200–300 MeV in the gamma spectrum, also seen as a broad distribution on the scatter plot at $M_{\pi^0}^2$, represents background from the three pion decays. Points concentrated at zero mass and low energy represent events with one gamma. To reduce the three-pion and collinear-events background, the cuts $-15000 \leq M_{inv}^2 \leq 15000$, $E_\gamma \leq 140 \text{ MeV}$ and $\Delta\phi \geq 0.03 \text{ rad}$ were applied. The sample of events, selected with the above cuts, still contained about 30% of $e^+e^- \rightarrow \mu^+\mu^-\gamma$ events.

The visible cross section of the processes $e^+e^- \rightarrow \mu^+\mu^-\gamma + \pi^+\pi^-\gamma$ vs. energy is presented in Fig. 8(a). With the cuts listed above, the detection efficiency of these processes, obtained by simulation, was found to be 0.17, leaving 1.7 nb of the visible cross section. The observed 20% difference from the average experimental cross section is due to the losses of the low-energy gammas, not correctly described by a simulation. The curve shows a theoretical prediction of the cross section including the influence of ϕ on the photon propagator (vacuum polarization) and

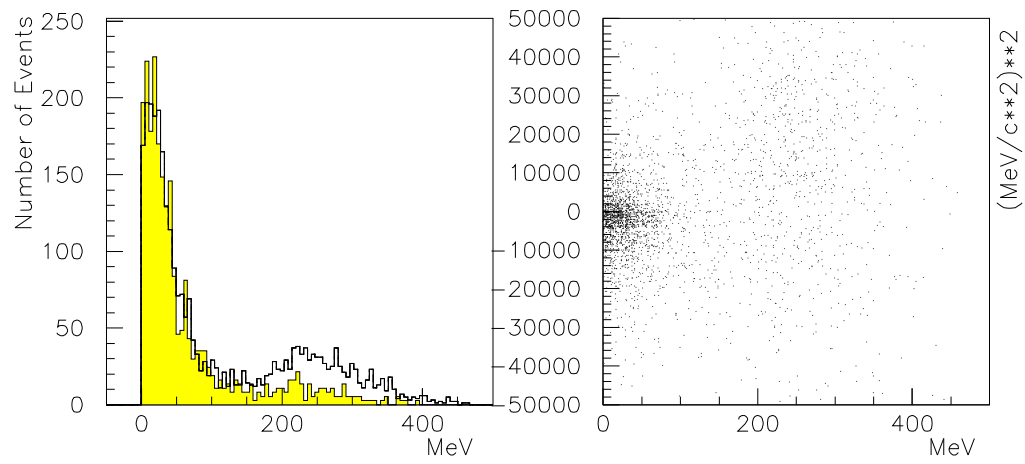


Fig. 7. Search for $\phi \rightarrow f_0\gamma$; (a) single gamma spectra (the shaded histogram represents the “non- ϕ ” region), and (b) the squared missing mass vs. photon energy.

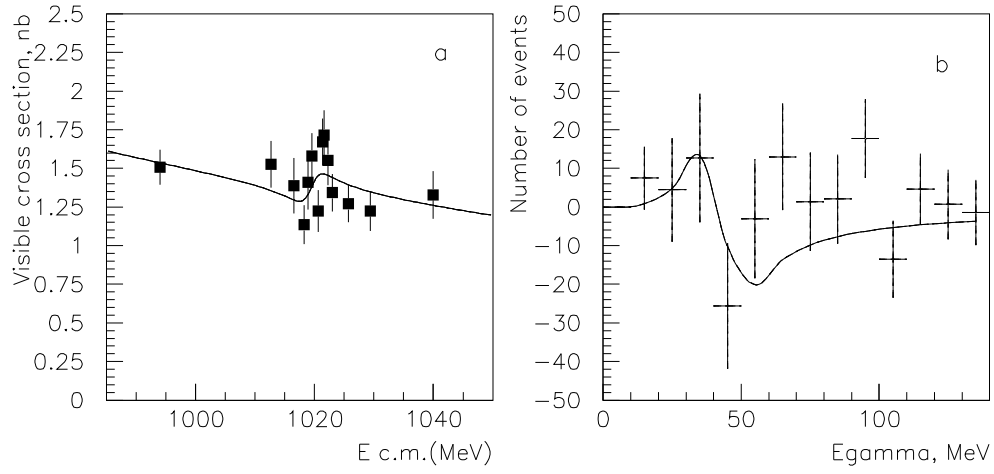


Fig. 8. $\phi \rightarrow f_0\gamma$ search. (a) Visible cross section for $e^+e^- \rightarrow \pi^+\pi^-\gamma + \mu^+\mu^-\gamma$ events. (b) Normalized difference in photon spectra. The curve is a prediction of the four-quark model with destructive interference and $B(\phi \rightarrow f_0\gamma) = 2.5 \times 10^{-4}$.

f_0 production, according to the Achasov four-quark model. The total branching ratio of $\phi \rightarrow \pi^+\pi^-\gamma$ could be extracted from this interference picture.

The signal from the decay of the $\phi \rightarrow f_0\gamma$ should be seen as a 30–40 MeV width structure at 45 MeV in the difference gamma spectra from the “ ϕ ” region and the “non- ϕ ” region shown in Fig. 8(b), together with the theoretical prediction calculated by the Achasov model for the four-quark state. With the present statistics, only an upper limit can be set.

Taking into account the effective number of ϕ 's 1.1×10^6 and all inefficiencies described above, the upper limit was found to be

$$B(\phi \rightarrow f_0\gamma) \leq 8.0 \times 10^{-4} \text{at} C.L. = 90\% \quad .$$

8 The K_L Nuclear Interaction as a Tag for K_S Rare Decay Study

K_L candidates are selected by looking at calorimeter clusters opposite a two-track vertex with an effective mass consistent with that of the kaon. Figure 9(a) shows the space angle between the predicted missing momentum direction of K_L and the cluster in the calorimeter. Figure 9(b) shows the energy deposition of the presumed K_L , Fig. 9(c) shows the number of hit crystals, and Fig. 9(d) shows the probability for a K_L to interact, corrected for the interaction in surrounding materials. The clusters from K_L are very broad and in 25% of the cases are split into two to four pieces. Simulated distributions are shown shaded. Comparison of the data with the GEANT simulation (using the GHEISHA package) shows definite disagreement. The difference is due to completely incorrect cross sections for the low-energy kaons, used by the GHEISHA package.

Once the properties of the K_L clusters are understood, one can use the K_L cluster as a “tag” for K_S decays. Figure 10(a) shows the invariant mass distribution for the events with two charged tracks opposite to K_L clusters.

The constrained fit applied to the decay $K_S \rightarrow \pi^+\pi^-$ extracted 32,340 events, which were used for normalization. The rest is shown in Fig. 10(a) as the shaded histogram. In order to search for the $\pi^+\pi^-\gamma$ mode, the sample of events with an acollinearity angle less than 2.4 radians, $M_{inv} \leq 450 \text{ MeV}/c^2$, and $E_\gamma \geq 50 \text{ MeV}$ was taken. Figure 10(b) shows the missing mass distribution for the two-track vertex, taking the K_S direction from the observed cluster, and the K_S momentum

Fig. 9. K_L interactions (dashed hits for simulation). (a) Space angle between calorimeter cluster and P_{mis} . (b) Energy deposition of K_L clusters. (c) Number of hit crystals (dashed hits for simulation). (d) Probability of K_L interactions in CsI.

from the known center-of-mass energy, and assuming $\phi \rightarrow K_S K_L$. 34.5 ± 8.0 events at zero mass, corresponding to the decay $K_S \rightarrow \pi^+ \pi^- \gamma$, were found after fitting and background subtraction. The simulated ratio of the acceptances for $K_S \rightarrow \pi^+ \pi^-$ and $K_S \rightarrow \pi^+ \pi^- \gamma$ was found to be 2.49 ± 0.30 , giving a branching ratio $\text{Br}(K_S \rightarrow \pi^+ \pi^- \gamma) = (1.82 \pm 0.49) \times 10^{-3}$.

Fig. 10. $K_S \rightarrow \pi^+ \pi^- \gamma$ search. (a) Invariant mass for vertices opposite clusters. Events without K_S decaying to two pions are shown shaded. (b) Missing mass in the frame of K_S . Events with real gammas found are shown shaded.

9 The $K_S K_L$ Coupled Decay Study

The event candidates were selected from a sample in which two vertices, each of two opposite charged tracks, were seen. An example of this kind of event is shown in Fig. 11.

Figures 12(a) and 12(b) show scatter plots of the invariant mass of the two charged tracks, assuming that they are pions, vs. missing momentum for the vertex closest to the beam and to the other one. The concentration corresponding to K_S 's dominates in Fig. 12(a) and is seen in Fig. 12(b). Two dimensional

Fig. 11. $\phi \rightarrow K_S K_L$ event with coupled decay.

cuts, $470 < M_{inv} < 525$ and $90 < P_{mis} < 130$ with an additional requirement to have another reconstructed vertex in the P_{mis} direction within detector resolution, select K_S 's in any of the vertices, with K_L 's remaining in the other. Figures 12(c) and 12(d) show a characteristic M_{inv} and P_{mis} broad distribution, expected from the main three-body K_L decays which are in good agreement with the simulation.

Figure 13(a) shows the distance from the point of origin to the decay point for selected K_S 's. An exponential decay length is seen with the correct value 0.58 ± 0.03 cm convoluted with vertex position resolution 0.23 cm.

Figure 13(b) shows the vertex radius for the K_L decays. A loss of efficiency for these events is seen, since the K_L events should be approximately flat in this spatial region corresponding to the very early part of the K_L lifetime. A significant peak with 59 ± 16 events is also seen and is interpreted as the nuclear interactions of K_L at the 0.077 cm Be vacuum beam pipe.

The histogram in Fig. 13(d) shows the events consistent with two-pion decay at the K_L vertices, when the additional cut in M_{inv} was applied. With our resolution, the suppression of the semileptonic K_L decays by a factor of 20 was expected, and these events dominated at all radii (only two CP-violating K_L decays were expected with the present sample), except for the beam pipe, where 28 ± 6 extra events survived. We interpret these events as regeneration of K_L into K_S .

The rest of the peak events may be explained by Σ and Λ production, when two pions are detected and the recoil nucleon is unseen. With the applied M_{inv}

cut, about 10% of these events may be interpreted as pure two-pion decays and should be extracted from the candidates for regenerated events.

Fig. 12. $K_S K_L$ coupled decay study. Invariant mass vs. missing momentum for (a) first and (b) second vertex. (c) Invariant mass for K_L and K_S (shaded) after K_S selection. (d) Missing momentum for K_L and K_S (shaded) after K_S selection.

Figure 13(c) shows the projected angle difference between the missing momentum direction and a line connecting the K_L vertex with the beam position, for the events concentrated around the beam pipe. Dots with errors show the expected distribution for semileptonic decays of K_L , normalized to the expected number of these events. A peak at zero angle is seen, supporting the hypothesis of K_L into K_S regeneration.

Taking into account 10% corrections for the DC mylar window and 10% from nuclear interaction background, the regeneration cross section is found to be $\sigma_{reg}^{Be} = 63 \pm 19$ mb. A visible nuclear interaction cross section (excluding regeneration) is found to be $\sigma_{nucl}^{Be} = 60 \pm 18$ mb.

The obtained regeneration cross section is in agreement with the calculations, performed in Frascati,³⁰ that gave a value 40 mb for 114 MeV/c long-lived kaons. For the total nuclear interaction cross section of neutral kaons, one can obtain a value 549 ± 165 mb, taking into account the ratio 0.21 of hyperon production to all other inelastic processes³¹ and 0.52 as the ratio of inelastic to elastic cross section.³⁰ It is also in good agreement with experimental data for higher momenta and the calculation of Ref. 30.

10 Study of $e^+e^- \rightarrow \pi^+\pi^-$

The data discussed in this talk were obtained by scanning the energy region between ϕ and ρ mesons with 10 MeV steps. About 1,000 pion pairs were sampled at every point. Most of the ~ 300 nb⁻¹ integrated luminosity was collected during the 1994 run. In the 1995 run, this work was continued below the ρ peak down to 600 MeV. Using the resonance depolarization technique,³² the beam energy at each point was measured with an accuracy of 10^{-4} . The detector trigger is described in Ref. 33. Events were recorded when:

- at least one track in the Drift Chamber was found by the tracking processor,³⁴ and
- the energy deposition in the CsI calorimeter was greater than 20 MeV.

About 20 million events were written onto magnetic tape. For off-line analysis, only collinear two-track events were selected. The cuts used for this selection are marked by arrows in Fig. 14. Events were used in a maximum likelihood function fit with the following global optimization parameters:

- number of electrons N_e ,
- number of background events N_b ,
- $\frac{N_\pi}{N_e + N_\mu}$, where N_π is the number of pions and N_μ is the number of muons.

The ratio N_μ/N_e was fixed from QED. The likelihood fit used information on the polar angle, longitudinal coordinate of the vertex, and energies deposited in the CsI calorimeter. As it is seen from Fig. 15, the experimental data are in good agreement with the fit.

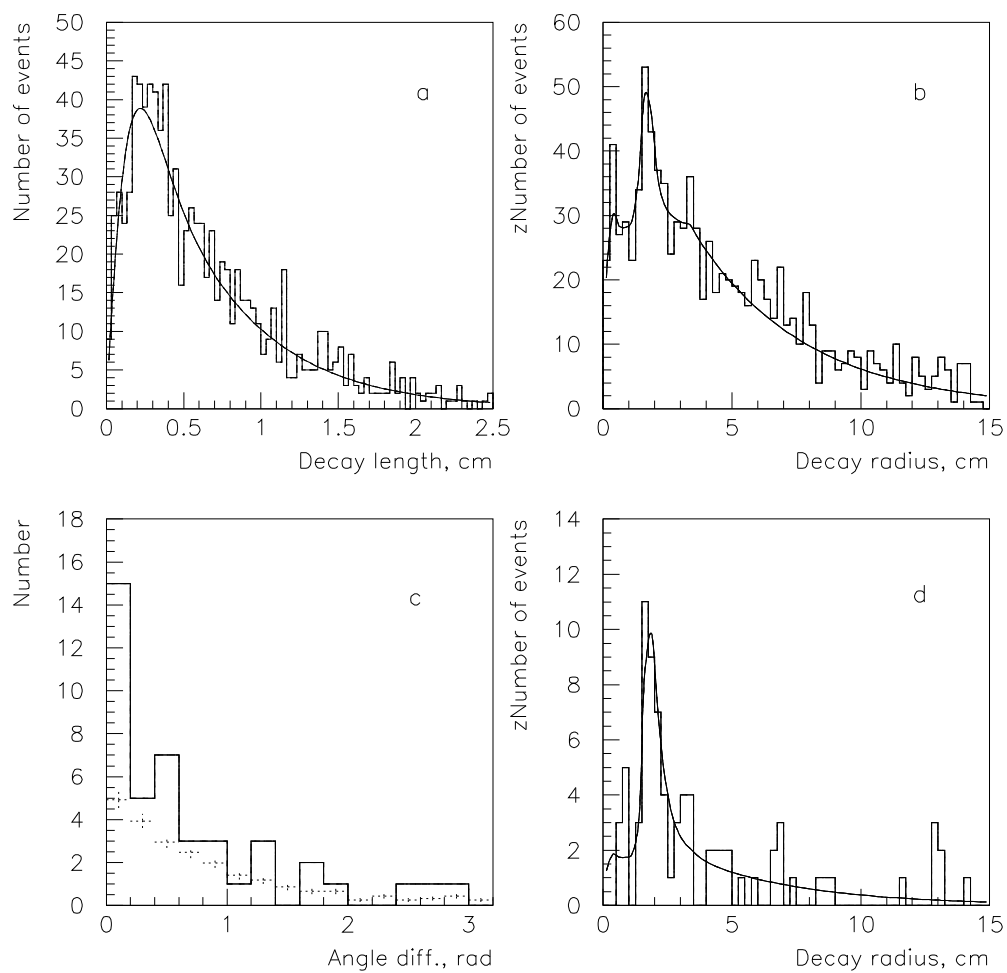


Fig. 13. $K_S K_L$ coupled decay study. (a) Decay length for K_S 's. (b) Decay radius for K_L 's. (c) Difference in angle of P_{mis} and the line from vertex to beam. (d) Decay radius for K_L 's after the M_{inv} cut; crosses are the expectation from K_L semileptonic decays.

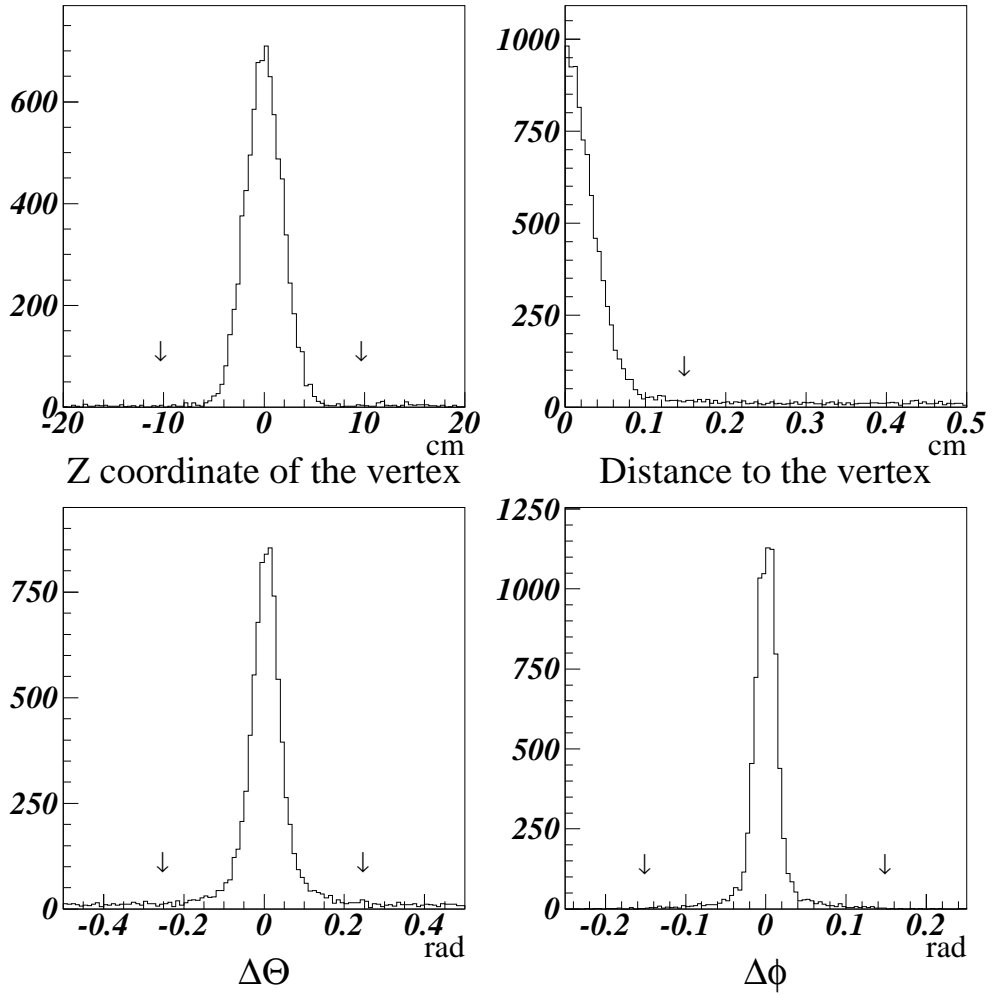


Fig. 14. Two-track event distributions and cuts imposed to select collinear events.

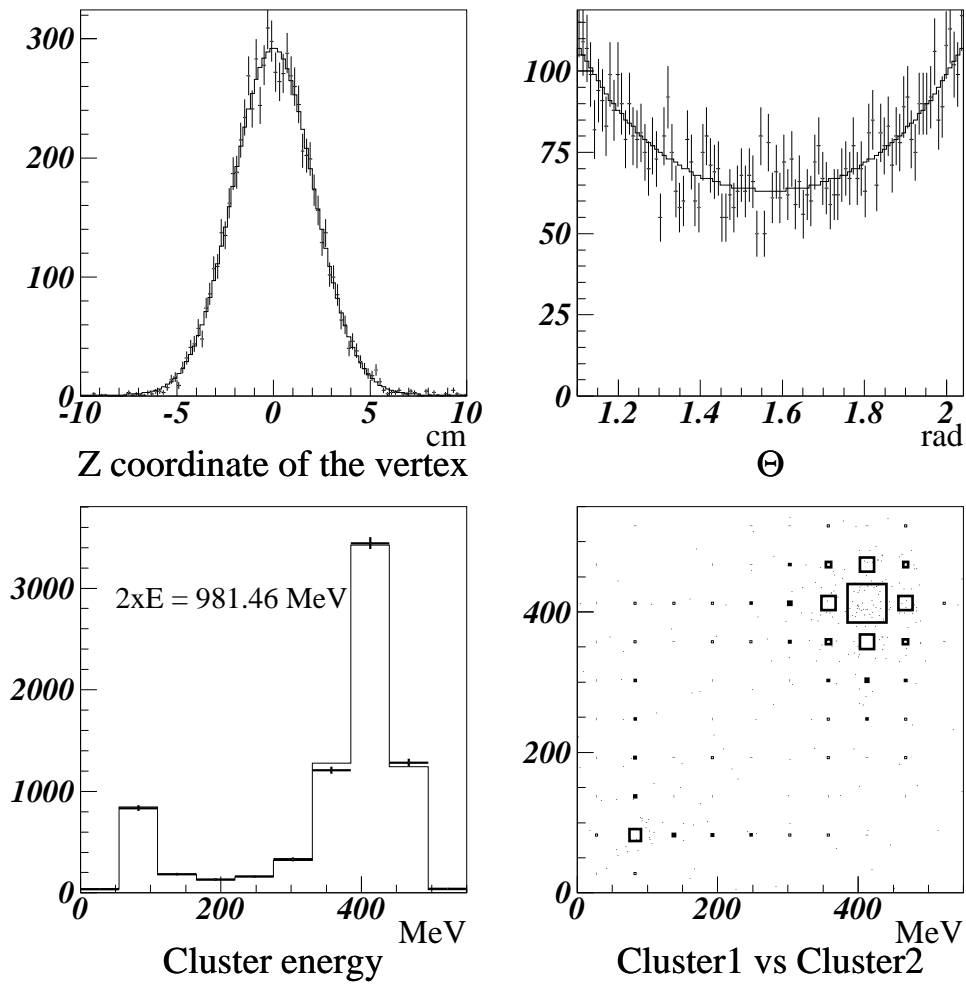


Fig. 15. The comparison of the experimental data with a fit.

The ratio $\frac{N_\pi}{N_e+N_\mu}$ allows us to express the $e^+e^- \rightarrow \pi^+\pi^-$ cross section in a simple way:

$$\sigma_\pi = \frac{N_\pi}{N_e + N_\mu} \cdot \frac{\epsilon_e \sigma_e (1 + \delta_e) + \epsilon_\mu \sigma_\mu (1 + \delta_\mu)}{\epsilon_\pi (1 + \delta_\pi)},$$

where $\epsilon_e, \sigma_e, \delta_e, \epsilon_\mu, \sigma_\mu, \delta_\mu, \epsilon_\pi, \sigma_\pi,$ and δ_π are detection efficiencies, cross sections, and radiative corrections for electrons, muons, and pions, respectively.

Pion form factor values are presented in Fig. 16 along with the results of the previous experiments. The statistical error of the $\pi^+\pi^-$ cross section at each energy point is less than 3%. At present, the total systematic error is estimated to be $\sim 1.5\%$. The main part of this error comes from the detector solid angle uncertainty $\sim 1\%$ and from the calculation of the radiative corrections for Bhabha events,³⁵ which are known with accuracy $\sim 1\%$.

The results from the OLYA detector have approximately the same statistical accuracy, whereas the systematical error in this energy range is about 4%.

Radiative corrections for all other channels of the e^+e^- annihilation into hadrons and muons were calculated with the accuracy about 0.2–0.5% (Refs. 36, 37) which is sufficient for the purposes of the experiment.

The Drift Chamber z -coordinate measurement can be calibrated by the Z chamber and thus improved significantly. Along with the more accurate calculations of the radiative corrections for Bhabha scattering events, this would decrease the systematic error to the level of 0.5%.

11 Conclusion

The next stage in this work is to process the data with improved detector resolution and to use all available particle identification information (drift chamber amplitudes, calorimeter energy deposition, and muon detector hits). The detector reconstruction efficiency is under intensive study and will reduce systematic errors for all results presented in this paper. Some other rare ϕ decay processes are under study.

The presence of regeneration and nuclear interaction background for the CP-violating decays of K_L will pose an additional background for ϕ -factory studies and should be under careful study.

Analysis of the collected data and new experimental runs are in progress, and we expect new results in the studies of ϕ, ω, ρ mesons and also in precision total hadronic cross-section measurements. The data taking at the ϕ is also planned with at least ten times more integrated luminosity before reconstruction of VEPP-

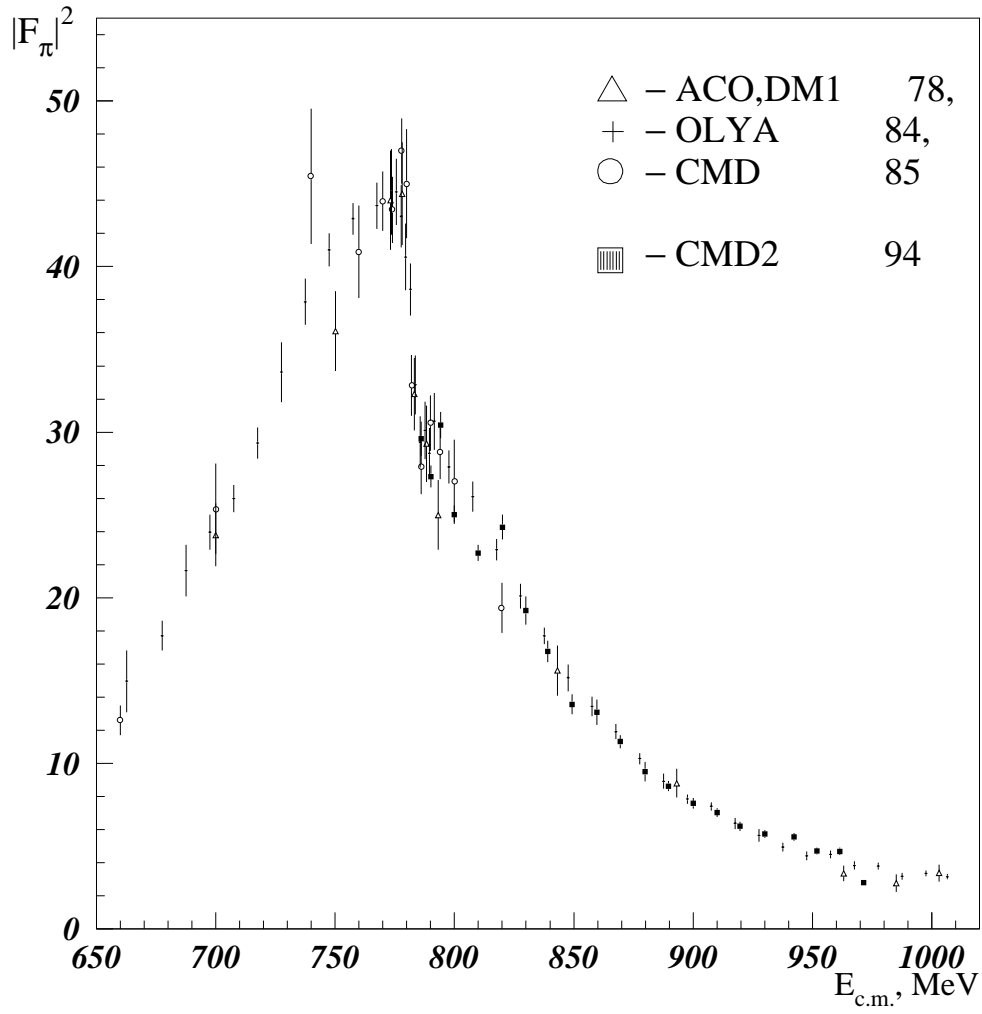


Fig. 16. The experimental data for $|F_\pi|^2$.

2M for round beam operation, which promises an additional factor of ten in the data sample.

Acknowledgments

I would like to thank R. Baldini and A. Michetti for their advice and useful discussions on the nuclear interaction study.

This work is supported in part by the U.S. Department of Energy, the U.S. National Science Foundation, and the International Science Foundation under grant RPT000.

References

- [1] V. V. Anashin *et al.*, preprint INP **84-114** (Novosibirsk, 1984).
- [2] L. M. Barkov *et al.*, Nucl. Phys. B **256**, 365 (1985).
- [3] A. D. Bukin *et al.*, Sov. J. Nucl. Phys. **27**, 516 (1978).
- [4] S. I. Dolinsky *et al.*, Phys. Rep. **202**, 99 (1991).
- [5] V. N. Bayer, ZETFP **17**, 446 (1973).
- [6] G. A. Aksenov *et al.*, preprint Budker INP 85-118 (Novosibirsk, 1985).
- [7] P. Eberhard, contribution to the ϕ Factory Workshop at UCLA, April 1990; G. Ghirardi, *Proceedings of the Workshop on Physics and Detectors for DAΦNE* (Frascati, April 1991), p. 261.
- [8] J. L. Rosner, I. Dunietz, and J. Hauser, Phys. Rev. D **35**, 2166 (1987).
- [9] A partial list of other major contributions include: A. N. Skrinsky *et al.*, “Novosibirsk ϕ -factory project”; F. J. Botella, J. Bernabeu, and J. Roldan-Blois, CP Violation Conference, FTUV/89-35, IFIC/89-11, May 1989; G. Barbiellini and C. Santoni, CERN-EP/89-8 and CERN-PPE/90-124; J. A. Thompson, University of Pittsburgh, preprint PITT-90-09; contributions by J. A. Thompson, D. Cline, C. Buchanan, and others to the ϕ Factory Workshop at UCLA, April 1990; Y. Fukushima *et al.*, KEK preprint 89-159; summary talks by P. Franzini and M. Piccolo and others at the Workshop on Physics and Detectors for DAΦNE, Frascati, April 1991.
- [10] A. N. Skrinsky, *Proceedings of the Workshop on Physics and Detectors for DAΦNE* (Frascati, April 1991), p. 67.

- [11] G. Vignola, *Proceedings of the Workshop on Physics and Detectors for DAΦNE* (Frascati, April 1991), p. 11.
- [12] A. N. Filippov *et al.*, *Proceedings of the XVth International Conference on High Energy Accelerators*, V. II (Hamburg, Germany, 1991, World Scientific), p. 1145.
- [13] S. Eidelman, E. Solodov, and J. Thompson, Nucl. Phys. B (Proceedings Supplement) A **24**, 174 (1991).
- [14] D. Cocolicchio *et al.*, Phys. Lett. B **238**, 417 (1990).
- [15] P. Franzini, *Proceedings of the Workshop on Physics and Detectors for DAΦNE* (Frascati, April 1991).
- [16] N. N. Achasov and V. N. Ivanchenko, Nucl. Phys. B **315**, 465 (1989).
- [17] S. Nussinov and T. N. Truong, Phys. Rev. Lett. **63**, 1349 (1989); A. A. Pivovarov, Soviet Physics—Levedev Institute Reports **9**, 12 (1990); N. Paver, contribution to ϕ Factory Workshop at UCLA, April 1990; J. L. Lucio and J. Pestieau, Phys. Rev. D **42**, 3253 (1990); and Oakes *et al.*, Phys. Rev. D **42** (1990).
- [18] F. Close, plenary talk at the Workshop on Physics and Detectors for DAΦNE, Frascati, April 1991; and F. E. Close, N. Isgur, and S. Kumano, Nucl. Phys. B **389**, 513 (1993).
- [19] S. Eidelman, J. A. Thompson, and C. H. Yang, *Proceedings of the Workshop on Physics and Detectors for DAΦNE* (Frascati, April 1991), p. 437.
- [20] The summary talks of L. Maiani and R. Baldini Ferroli, of N. N. Achasov, and of M. Pennington at the Workshop on Physics and Detectors for DAΦNE, Frascati, April 1991.
- [21] M. Vysotski, plenary talk, *Proceedings of the XXVII Int. Conf. on High-Energy Physics* (1993).
- [22] Muon g-2 Design Report, AGS 821, BNL (July 1992).
- [23] S. Eidelman and F. Jegerlehner, Z. Phys. C **67**, 585 (1995).
- [24] E. V. Anashkin *et al.*, ICFA Instrumentation Bulletin **5**, 18 (1988).
- [25] R. R. Akhmetshin *et al.*, preprint Budker INP 95-35, Novosibirsk, 1995.
- [26] J. Lee-Franzini *et al.*, Phys. Lett. B **287**, 259 (1992).
- [27] A. Bramon *et al.*, Phys. Lett. B **287**, 263 (1992).

- [28] J. Lee-Franzini *et al.*, DAΦNE Physics Handbook, V.II (Frascati, 1992), p. 513.
- [29] L. Montanet *et al.*, Phys. Rev. D **50**, 1173 (1994).
- [30] A. Michetti, Thesis, Roma University, 1993.
- [31] This value was extracted from the NUCRIN package.
- [32] Y. S. Derbenev *et al.*, Part. Acc. **10**, 177 (1980).
- [33] E. V. Anashkin *et al.*, Nucl. Instrum. Methods A **323**, 178 (1992).
- [34] V. M. Aulchenko *et al.*, Nucl. Instrum. Methods A **252**, 299 (1986).
- [35] F. A. Berends and R. Kleiss, Nucl. Phys. B **228**, 537 (1983).
- [36] E. A. Kuraev and V. S. Fadin, Sov. J. Nucl. Phys. **41**, 466 (1985).
- [37] S. I. Eidelman *et al.*, preprint Budker INP 95-34, Novosibirsk, 1995.
- [38] F. A. Berends and G. J. Komen, Phys. Lett. B **63**, 432 (1976).